Nuclear Engineering and Technology 53 (2021) 927–931

Contents lists available at ScienceDirect

Nuclear Engineering and Technology

journal homepage: www.elsevier.com/locate/net

Original Article

Electrochemical corrosion study of helium ions implanted Zircaloy-4 in chloride media

Mohsin Rafique [a, *], Atika Khan [a], Naveed Afzal [a], Ameeq Farooq [b], M. Imran [c]

[a] Centre for Advanced Studies in Physics, GC University, Lahore, Pakistan
[b] Corrosion Control Research Cell, Department of Metallurgy and Materials Engineering, CEET, University of the Punjab, Lahore, Pakistan
[c] Department of Physics, GC University, Lahore, Pakistan

ARTICLE INFO

Article history:
Received 6 February 2020
Received in revised form
24 July 2020
Accepted 3 August 2020
Available online 8 August 2020

Keywords:
Zircaloy-4
Helium ions
Potentiodynamic polarization
Corrosion rate
Current density

ABSTRACT

In this work, an attempt is made to improve the electrochemical corrosion resistance of Zircaloy-4 by helium ions implantation. For this purpose, the Zircaloy-4 was implanted with 300 keV helium ions of fluences 1×10^{13}, 1×10^{15}, and 1×10^{16} ions-cm^{-2} by using Pelletron Accelerator. Electrochemical tests of pristine and ion-implanted samples were performed in NaCl solution and their potentiodynamic polarization curves were obtained. The results showed enhancement of the corrosion resistance of Zircaloy-4 after helium ions implantation. The corrosion rate and current density of the material were significantly reduced by the helium implantation. The decrease in corrosion parameters was attributed to helium ions diffusion inside Zircaloy-4 that reduced the electrons flow from the samples.

1. Introduction

Zircaloy-4 is an alloy of zirconium and tin (Zr–Sn) that finds application in the confinement of nuclear reactor fuel as well as it is used in the structural parts of the Pressurized Water Reactors (PWRs). Zircaloy-4 exhibits high mechanical strength along with a good chemical stability in aggressive environments [1,2]. However, the waterside corrosion of Zircaloy-4 causes the formation of an oxide layer on its surface that degrades its mechanical stability with time [3]. Furthermore, hydrogen incorporation in Zircaloy-4 results in the formation of hydrides that accelerate its corrosion rate [4]. Therefore, the oxidation of Zr alloys and the associated hydrogen pickup must be avoided to prevent these from the corrosion [5].

Ion implantation is well-known technique that is often used to improve the corrosion resistance and hardness of metals and alloys [6]. Ion implantation in metallic material may produce structural defects such as vacancies and interstitials that modify their surface properties [7–11]. Significant effort has been made to study radiation effects in Zr alloys used in nuclear reactors. It has been found that the fast neutron interaction with the structural components of a nuclear reactor results in the formation of helium ions through the (n, α) reaction [12–14]. Due to low solubility in metals, the helium atoms are captured by the grain boundaries, vacancies, and dislocations that affect the corrosion rate of Zircaloy-4. Previous studies showed that the implantation of inert gas ions such as helium significantly affect the surface and structural properties of nuclear materials [15–19]. Yoshida et al. [17] investigated the impact of low energy helium ions on the microstructure and surface properties of Tungsten. The dense and fine bubbles of helium along with the dislocation loops were formed in Tungsten at low temperature. The hardness of the material was increased due to the formation of helium bubbles. Soria and co-workers [18] studied the effect of 20 keV helium ions irradiation on the microstructure of Al and Al–Cu alloy at 1.5×10^{17} ions.cm^{-2}. The results showed homogeneous blistering and small helium bubbles (of 1–2 nm diameter) in pure Al whereas no bubble formation was observed in the irradiated Al–Cu alloy. The post-irradiation annealing of the irradiated Al alloy caused the formation of uniformly distributed helium bubbles. Recently, our group studied the impact of 300 keV helium ions on the structural characteristics of Zircaloy-4 at various doses. The crystallinity of Zircaloy-4 decreased after helium irradiation at lower doses due to the radiation damage whereas it was improved at 1×10^{16} ions-cm^{-2} due to thermal effects of irradiation [19]. This work is an expansion of our recent work as stated above. In this work, electrochemical corrosion of 300 keV helium ions

* Corresponding author.
E-mail address: mohsinrafique@gcu.edu.pk (M. Rafique).

https://doi.org/10.1016/j.net.2020.08.004

implanted Zircaloy-4 has been investigated at various ion fluences. The objective is to study the changes in the electrochemical corrosion parameters of Zircaloy-4 due to helium ions implantation in it.

2. Experimental procedure

Square shaped samples of Zircaloy-4 were cut with the dimensions of 1×1 cm^2 from the as-received sheet having a thickness of 0.5 mm. The chemical composition of this alloy contains Sn (1.32%), Fe (0.21%), Cr (0.11%), C (0.014%), Si (0.0093%), O (0.12%) and balanced Zr. All the samples were abraded with emery papers of different grit sizes and then polished by using a diamond paste of 10 and 6 μm grade to give it a mirror finish. After polishing, helium ions (He^+) implantation in Zircaloy-4 was conducted at various doses such as 1×10^{13}, 1×10^{15}, and 1×10^{16} ions-cm^{-2} at room temperature. The Pelletron Accelerator installed at GCU, Lahore was used for irradiation of Zircaloy-4 [19]. An image of the Pelletron Accelerator used in this work is shown in Fig. 1. The radiofrequency (RF) ion source was used to obtain helium ions. For this purpose, helium plasma was produced using the RF ion source. The negative helium ions were extracted from the helium gas plasma through the RF source and were accelerated towards the Pelletron tank by applying voltage where these were converted into positive helium ions through gas stripping. These ions were then focused on the sample for the irradiation purpose through the electrostatic potential difference. The ion dose was varied by changing the irradiation time while the ion energy was kept constant at 300 keV. The helium ions range inside Zircaloy-4, calculated using Stopping and Range of Ions in Matter (SRIM) software, was 0.84 μm [19]. The potentiodynamic polarization technique was used to determine the electrochemical response of pristine and ion-implanted Zircaloy-4. The samples were fixed on a copper holder for an electrical connection while all sides of the samples were insulated with epoxy with an exposed surface area of 1 cm^2. For the electrochemical testing, the three electrodes system coupled with potentiostat (Gamry 1000E, USA) was used. The pristine and ion-implanted samples were used as working electrodes. The Ag/AgCl (sat. KCl) and graphite were treated as reference and counter electrodes respectively. A schematic diagram of the electrochemical setup used in this work is presented in Fig. 2. The corrosion potential, current density and corrosion rate were determined from the polarization curves. The acidic solution of 17 mM NaCl having pH 3 (adjusted by 0.1 N HCl solution) was used as electrolyte. The temperature of the system was maintained at 35 °C by using thermostatic circulating bath. The samples were immersed in an electrolyte for one hour to obtain a stable open circuit potential (OCP). After stabilization, the samples were polarized cathodically to a fixed potential of −0.5 V vs OCP while polarized anodically to a fixed potential of +1.5 V vs OCP with a scan rate of 1 mV/s. The corroded surfaces were also examined by using scanning electron microscope (SEM). The results were analyzed and compared.

3. Results and discussion

The polarization curves of pristine and helium ion implanted samples are shown in Fig. 3. These curves were Tafel fitted to determine corrosion current density (i_{corr}), corrosion potential (E_{corr}) and corrosion rate of Zircaloy-4 as given in Table 1. The polarization curves show both anodic and cathodic branches that indicate the dissolution of the material at high potential and hydrogen evolution through the reduction reaction [20,21]. The E_{corr} value for the pristine sample is −190 mV which is shifted to a more negative value of −250 mV after helium ions implantation at 1×10^{13} ions-cm^{-2}. The helium ion implantation in Zircaloy-4 produces structural defects that may also affect its surface properties. As a result of the surface modification, the E_{corr} value becomes more negative. However, at 1×10^{15} ions-cm^{-2}, the E_{corr} value becomes less negative −215 mV, which further decreases to −186 mV with increasing the ion fluence to 1×10^{16} ions-cm^{-2}. This is attributed to the thermal effects of irradiation at higher doses that minimize the structural/surface defects as explained in our previous work [19]. During cathodic polarization, the pristine sample shows a bend in the curve, which may be due to its greater tendency to adsorb hydrogen atoms (H_{ads}) for the acidic solution followed by the hydrogen gas evolution as demonstrated by the following reactions;

$$H^+ (aq) + e^- \rightarrow H_{ads} \quad (1)$$

Fig. 1. Image of Pelletron Accelerator used for Irradiation.

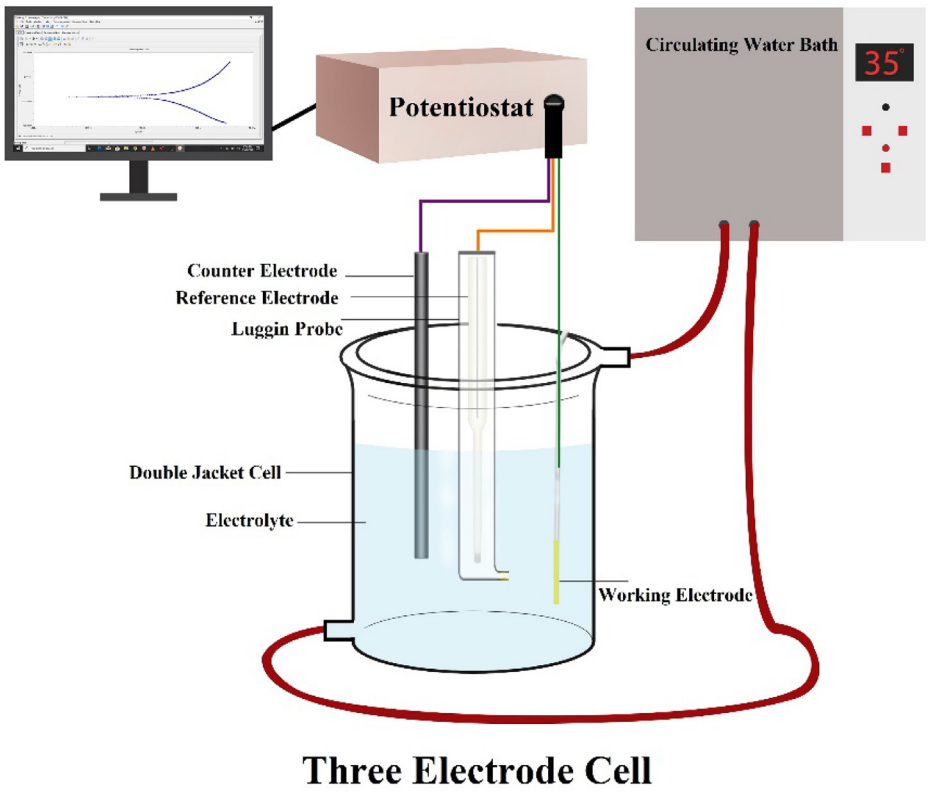

Fig. 2. Schematic diagram of electrochemical setup.

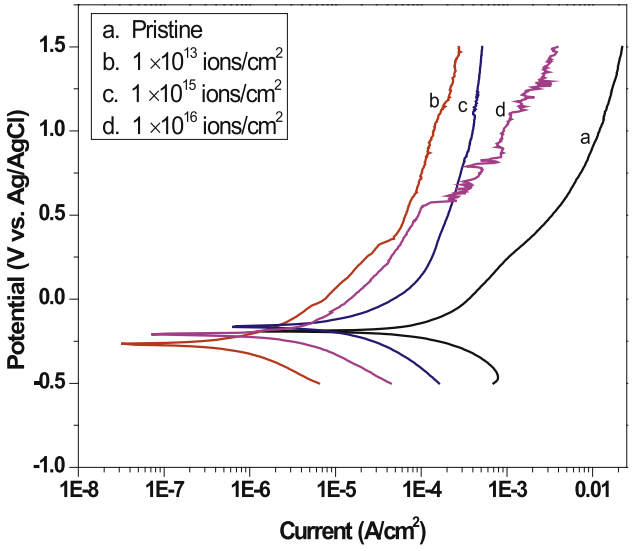

Fig. 3. Comparison of potentiodynamic polarization curves of unimplanted and helium ion (He^+) implanted Zircaloy-4 Alloy.

$$H_{ads} + H_{ads} \rightarrow H_2\,(g) \quad (2)$$

Zirconium and its alloys develop hydrogen gas bubbles during cathodic polarization in an acidic solution as reported in previous studies [22,23]. These show good resistance to corrosion in water, however, when a small amount of chloride or fluoride ions are present in water, then the corrosion resistance of Zr alloys decreases. This is due to the de-polarizer nature of the chloride/fluoride ions that cause damage to the protective oxide layer. This phenomenon becomes stronger when the pH of the water is on the acidic side [23–25].

In this work, when the pristine sample of Zircaloy-4 was polarized anodically, then the dissolution reaction was initiated and this extended the activation polarization region towards the high current density value (240 μA cm^{-2}). Consequently the corrosion rate of the sample was increased (112.5 mpy). The absence of the active nose in the polarization curve indicates that there is no passive film formation during the anodic polarization. According to the previous literature, the protective passive film on zirconium and its alloy (ZrO_2) is dissolved into ZrO^{2+}, when the solution pH is lesser than or equal to 3.5 according to the following reaction [22]:

Table 1
Kinetic parameters calculated from potentiodynamic polarization.

Parameters	Units	Pristine	1×10^{13} ions-cm^{-2}	1×10^{15} ions-cm^{-2}	1×10^{16} ions-cm^{-2}
i_{corr}	μA.cm^{-2}	240	13.70	10.70	1.99
E_{corr}	mV	−190	−250	−212	−186
Corrosion Rate	mpy	112.5	6.412	5.013	0.932

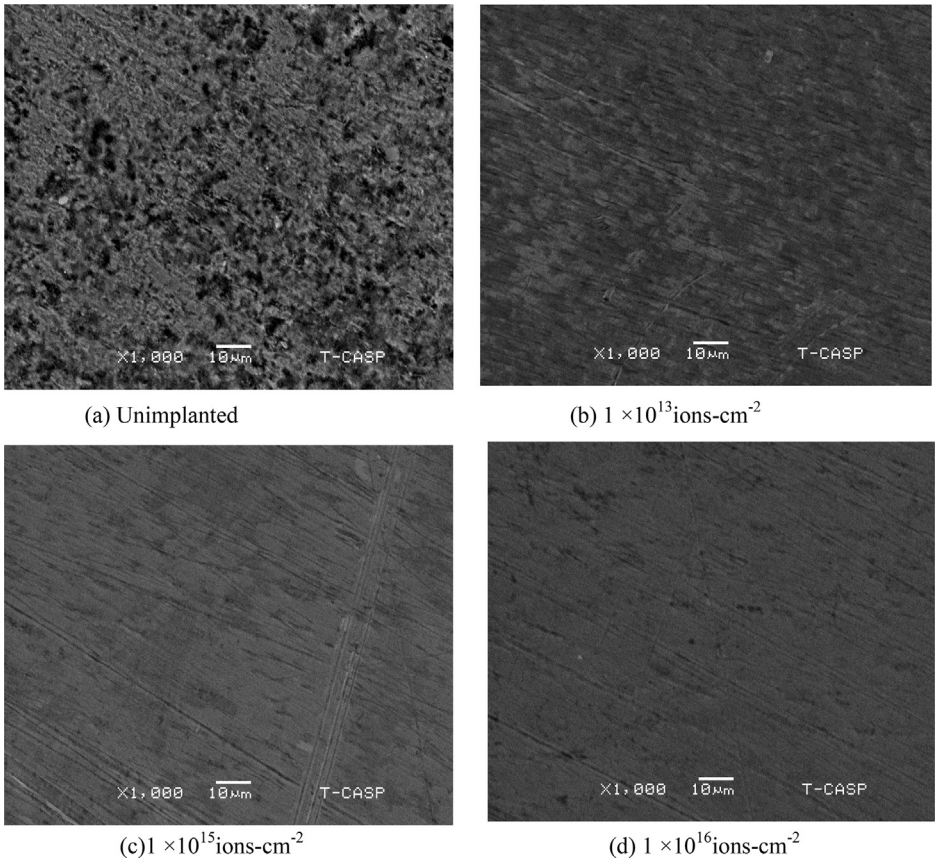

(a) Unimplanted (b) 1 ×10^{13}ions-cm^{-2}

(c)1 ×10^{15}ions-cm^{-2} (d) 1 ×10^{16}ions-cm^{-2}

Fig. 4. (a–d) SEM images of corroded Zircaloy-4 surface before and after helium ions implantation.

$$ZrO_2\,(s) + 2H^+\,(aq) \rightarrow ZrO^{2+}(aq) + H_2O\,(aq) \quad (3)$$

With the further decrease in the pH value below 3.5, the ZrO^{2+} are further converted into Zr^{+4} as depicted by the following reaction [22].

$$ZrO^{2+}\,(aq) + 2H^+\,(aq) \rightarrow Zr^{4+}(aq) + H_2O\,(aq) \quad (4)$$

The above reaction is much slower than the zirconium dissolution reaction which is given as;

$$Zr\,(s) \rightarrow Zr^{4+}(aq) + 4\,e^- \quad (5)$$

The Zr^{4+} ions hydrolyze and form zirconium hydroxyl ions ($ZrOH^{3+}$) which decrease the dissolution rate of the Zircaloy-4. The $ZrOH^{3+}$ further react with Cl^- ions present in the electrolyte and promotes the formation of hydrolyzed species $Zr\,(OH)\,Cl_2^+$. All these processes are presented through the following reactions [26];

$$Zr^{4+}(aq) + H_2O\,(aq) \rightarrow Zr(OH)^{3+}(aq) + H^+(aq) \quad (6)$$

$$Zr(OH)^{3+}(aq) + 4Cl^-\,(aq) \rightarrow Zr(OH)Cl^{2+}(aq) \quad (7)$$

When the helium ions are implanted in Zircaloy-4 at lower fluence (1×10^{13} ions-cm^{-2}) then the i_{corr} value decreases that also results in a decrease in the corrosion rate. The anodic polarization curve of the ion implanted sample (1×10^{13} ions-cm^{-2}) shows that the current density does not rise sharply with an increase of the applied voltage, indicating enhancement of the corrosion resistance of Zircaloy-4. The corrosion rate further decreases as the helium ion fluence is increased up to 1×10^{16} ions-cm^{-2}. The value of corrosion rate at this dose is found to be 0.932 mpy. The decrease of the corrosion rate indicates a decrease in the dissolution of Zircaloy-4 in the acidic saline solution as compared to the pristine sample. This improvement occurs due to the diffusion of helium ions that react against the flow of electrons from the Zircaloy-4. These ions capture electrons and are converted into helium gas. This decreases the corrosion rate of the samples which becomes more prominent at higher doses due to greater diffusion of helium ions inside the material.

Fig. 4 shows the SEM surface morphology of Zircaloy-4 samples before and after corrosion testing in the NaCl solution. Fig. 4(a) represents the surface appearance of an un-implanted Zircaloy-4 sample whereas Fig. 4(b–d) presents the Zircaloy-4 samples implanted with helium ions at various irradiation fluences of 1×10^{13}, 1×10^{15} and 1×10^{16} ions-cm^{-2}. From the figures, it can be deduced that the pitting corrosion in the un-implanted sample is more pronounced as compared to ion-implanted samples. This pitting corrosion is due to the chloride ions (Cl^-) formed due to the ionic dissolution of NaCl in water, present on the Zircaloy-4 surface. When the helium ions are implanted in the Zircaloy-4, then the pitting density is reduced. When the helium fluence was increased to 1×10^{16} ions-cm^{-2}, the pitting on Zircaloy-4 surface was substantially decreased as shown in Fig. 3 (d). This shows that the alloy offer greater resistance against corrosion when implanted with helium ions. The results of corrosion morphology are in accordance with those from potentiodynamic polarization measurements.

4. Summary

Helium ions implantation in Zircaloy-4 improves its corrosion resistance. The corrosion current density and corrosion rate of Zircaloy-4 decrease with the increase of helium ion fleunce up to 1×10^{16} ions-cm^{-2}. The decrease in corrosion rate and current density is attributed to the diffusion of helium ions inside the Zircaloy-4 that reduces the oxidation of the sample. The value of corrosion potential becomes more negative at lower ion fluence (1×10^{13} ions-cm^{-2}) whereas it becomes more positive when the ion fluence is increased to 1×10^{16} ions-cm^{-2}. The pitting corrosion of Zircaloy-4 also significantly decreases after the helium ions implantation in it.

Declaration of competing interest

The authors declare that they have no known competing financial interests or personal relationships that could have appeared to influence the work reported in this paper.

Appendix A. Supplementary data

Supplementary data to this article can be found online at https://doi.org/10.1016/j.net.2020.08.004.

References

[1] B. Cox, J. Nucl. Mater. 336 (2005) 331–368.
[2] A. Sarkar, K.L. Murty, J. Nucl. Mater. 456 (2015) 287–291.
[3] A.T. Motta, JOM 63 (2011) 59–63.
[4] B. Ensor, A.M. Lucente, M.J. Frederick, J. Sutliff, A.T. Motta, J. Nucl. Mater. 496 (2017) 301–312.
[5] P. Platt, E. Polatidis, P. Frankel, M. Klaus, M. Gass, R. Howells, M. Preuss, J. Nucl. Mater. 456 (2015) 415–425.
[6] P. Sioshansi, Mater. Sci. Eng. 90 (1987) 373–383.
[7] A.T. Motta, A. Paesano Jr., R.C. Birthcher, L. Amaral, Nucl. Instr. Method B 175–177 (2001) 521–525.
[8] A.I. Ryabchikov, E.B. Kashkarov, N.S. Pushilina, M.S. Syrtanov, A.E. Shevelev, O.S. Korneva, A.N. Sutygina, A.M. Lider, Appl. Surf. Sci. 439 (2018) 106–112.
[9] A.I. Ryabchikov, E.B. Kashkarov, A.E. Shevelev, M.S. Syrtanov, Surf. Coat. Tech. 383 (2020) 125272.
[10] N. Afzal, M. Rafique, A. Abbasi, R. Ahmad, M. Saleem, J.M. Lee, Phys. Scripta 93 (2018) 115303.
[11] M. Rafique, N. Afzal, A. Farooq, R. Ahmad, Mater. Res. Exp. 5 (2018) 106501.
[12] I.R. Briss, J. Nucl. Mater. 34 (1970) 241–259.
[13] P.J. Goodhew, Inert gas bubbles, Mater. Sci. Tech. 6 (1990) 950–952.
[14] G.S. Was, Fundaments of Radiation Materials Science: Metals and Alloys, Springer-Verlag, Berlin, 2007.
[15] Gregory De Temmerman, K. Bystrov, J.J. Zielinski, J. Vac. Sci. Technol. A 30 (2012), 041306-1-7.
[16] H.H. Shen, S.M. Peng, B. Chen, F.N. Naab, G.A. Sun, W. Zhou, X. Xiang, K. Sun, X.T. Zu, Mater. Char. 107 (2015) 309–316.
[17] N. Yoshida, H. Iwakiri, K. Tokonaga, T. Baba, J. Nucl. Mater. 337–339 (2005) 946–950.
[18] S.R. Soria, A.J. Tolley, E.A. Sánchez, Procedia Mater. Sci. 8 (2015) 486–493.
[19] A. Khan, M. Rafique, N. Afzal, Z. Khaliq, R. Ahmad, Nucl. Mater. Energy 20 (2019) 100690.
[20] Robert G. Kelly, John R. Scully, David W. Shoesmith, Rudolph G. Buchheit, Electrochemical Techniques in Corrosion Science and Engineering, Marcel Dekker, Inc., New York, 2002, pp. 80–84.
[21] N.G. Thompson, J.H. Payer, Corrosion Testing Made Easy: DC Electrochemical Test Methods, NACE International, 1998.
[22] Marcel Pourbaix, Atlas of Electrochemical Equilibria in Aqueous Solution, National Association of Corrosion Engineers, USA, 1974.
[23] T.-L. Yau, V.E. Annamalai, Corrosion of zirconium and its alloys, Shreir's Corrosion 3 (2010) 2104–2107.
[24] D.R.I. Robert, H. Heidersbach, ASM Handbook: Corrosion Fundamentals, Testing and Protection, 13A, ASM International, 2003.
[25] P.R. Roberge, Handbook of Corrosion Engineering, McGraw-Hill, New York, 1999.
[26] Lipika Rani Bairi, S. Ningshen, U. Kamachi Mudali, Baldev Raj, Corrosion Sci. 52 (2010) 2299.